DALTON
FULL PAPER

The interconversion of formic acid and hydrogen/carbon dioxide using a binuclear ruthenium complex catalyst

Yuan Gao,[a] Joshi K. Kuncheria,[a] Hilary A. Jenkins,[a] Richard J. Puddephatt *[a] and Glenn P. A. Yap[b]

[a] *Department of Chemistry, University of Western Ontario, London, Ontario, Canada N6A 5B7*
[b] *Department of Chemistry, University of Ottawa, Ottawa, Ontario, Canada*

Received 26th May 2000, Accepted 25th July 2000
Published on the Web 23rd August 2000

The complex $[Ru_2(\mu\text{-}CO)(CO)_4(\mu\text{-}dppm)_2]$ in acetone solution is an efficient catalyst for the reversible reaction between formic acid and hydrogen/carbon dioxide. Complexes identified during the catalytic reactions include the hydrido and formato complexes $[Ru_2(\mu\text{-}H)(\mu\text{-}CO)(CO)_4(\mu\text{-}dppm)_2]^+$, $[Ru_2(\mu\text{-}HCO_2)(CO)_4(\mu\text{-}dppm)_2]^+$, $[Ru_2(\mu\text{-}H)_2(CO)_4(\mu\text{-}dppm)_2]$, $[Ru_2H(HCO_2)(CO)_4(\mu\text{-}dppm)_2]$ and the coordinatively unsaturated $[Ru_2H(\mu\text{-}H)(\mu\text{-}CO)(CO)_2(\mu\text{-}dppm)_2]$.

Introduction

The reversible reaction between HCOOH and $H_2 + CO_2$ has been the subject of considerable interest, either for catalytic transfer hydrogenation using formic acid as the hydrogen source[1–3] or for utilization of CO_2 as a reagent in organic synthesis.[4,5] There is a relationship with the Water Gas Shift reaction, as shown in eqn. (1). The formation of formic acid is

$$H_2O + CO \rightleftharpoons H_2 + CO_2 \rightleftharpoons HCO_2H \qquad (1)$$

unfavourable under normal conditions, but can be observed under high pressure in the presence of base.

The best homogeneous catalysts are more efficient than known heterogeneous catalysts for the hydrogenation of CO_2 to formic acid, as well as for the reverse reaction, and reaction mechanisms have been proposed in some cases.[5–8] Representative examples of mechanisms for formation of formic acid are shown in Scheme 1, and the decomposition will occur by the microscopic reverse. In mechanisms **A** and **B** of Scheme 1, the reagents add in the sequence CO_2 then H_2, while the reverse order is followed in mechanism **C**. A high degree of coordinative unsaturation is required for mechanism **A** since both steps require a vacant site at the metal; 14-electron complexes such as [RhH(diphosphine)] show high activity.[5,7] If the complex is coordinatively saturated, ligand dissociation might occur to allow mechanism **A**, or direct hydride transfer to CO_2 might occur as in mechanism **B**; this mechanism is proposed for the catalyst $[RhH(diphosphine)_2]$.[5] Finally, mechanism **C** is analogous to the mechanism commonly invoked for hydrogenation of alkenes; the catalyst $[Rh(PMe_2Ph)_3(solv)]^+$ is thought to operate by this type of cycle.[8] The proposed formate intermediates may be ionic (mechanism **B**), monodentate (mechanism **C**) or bidentate (mechanism **A**), and these bonding forms may easily interconvert.[4–8] Most mechanistic suggestions involve oxidative addition and reductive elimination cycles (Scheme 1) but hydrogenolysis of metal formate to formic acid might also occur directly from a dihydrogen complex intermediate.[7] Overall, although the reactions appear simple, there are several possible mechanisms and it is often difficult to distinguish between them.[4,5]

This paper reports a study of the catalysis of the reversible reaction of formic acid to carbon dioxide and hydrogen by the binuclear complex $[Ru_2(\mu\text{-}CO)(CO)_4(\mu\text{-}dppm)_2]$. It is remarkable that no other binuclear homogeneous catalyst has been found to be directly involved in either the decomposition of formic acid or the hydrogenation of CO_2 to formic acid. A preliminary report of the part of the work on catalytic decomposition of formic acid has been published.[9]

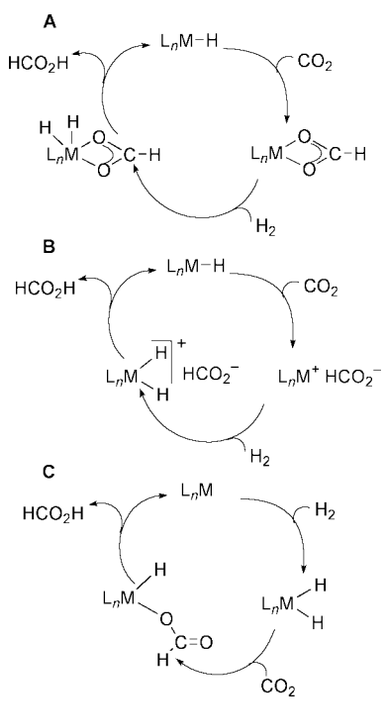

Scheme 1

Results

The reactivity of $[Ru_2(\mu\text{-}CO)(CO)_4(\mu\text{-}dppm)_2]$ toward formic acid

The decomposition of formic acid could be monitored by NMR spectroscopy. Thus, when excess ^{13}C labelled formic acid was added to a saturated solution of $[Ru_2(\mu\text{-}CO)(CO)_4(\mu\text{-}dppm)_2]$,**1**, in acetone-$d_6$ in an NMR tube at room temperature, and the NMR spectrum was recorded after 20 minutes, no formic acid remained but a sharp singlet at $\delta = 4.5$ due to H_2

 DOI: 10.1039/b004234j

was observed in the ^{1}H NMR spectrum and a strong singlet at $\delta = 126$ due to CO_2 was observed in the ^{13}C NMR spectrum. When the reaction was complete, the only ruthenium complex present in solution was complex **1**, identified by its ^{1}H and ^{31}P NMR spectra.[10] The formation of hydrogen and carbon dioxide was confirmed by mass spectrometry; no other products, notably the potential products CO and H_2O (eqn. (1)), were detected by NMR or MS. The turnover frequency of this reaction, when the initial concentrations of formic acid and **1** were 0.35 M and 2.2×10^{-3} M respectively, was *ca.* 500 h^{-1} at room temperature, indicating high reactivity compared to known mononuclear complex catalysts.[8,11] For example, $[RuHBr(CO)(PEt_2Ph)_3]$ gives a turnover frequency of 4 h^{-1} in refluxing acetic acid at 117 °C.[11] There is also an interesting contrast with the similar complex $[Ru_2(\mu\text{-}CO)(CO)_4\{\mu\text{-}(RO)_2PN(Et)P(OR)_2\}_2]$ which reacts only stoichiometrically and reversibly with formic acid to give the protonation product $[Ru_2(\mu\text{-}H)(\mu\text{-}CO)(CO)_4\{\mu\text{-}(RO)_2PN(Et)P(OR)_2\}_2]^+HCO_2^-$ (R = Et or *i*-Pr).[12]

The complexes identified in the catalytic reactions

To understand the decomposition mechanism, the reacting solution was monitored at low temperature by NMR spectroscopy in a sealed tube. A summary of the results is in Scheme 2

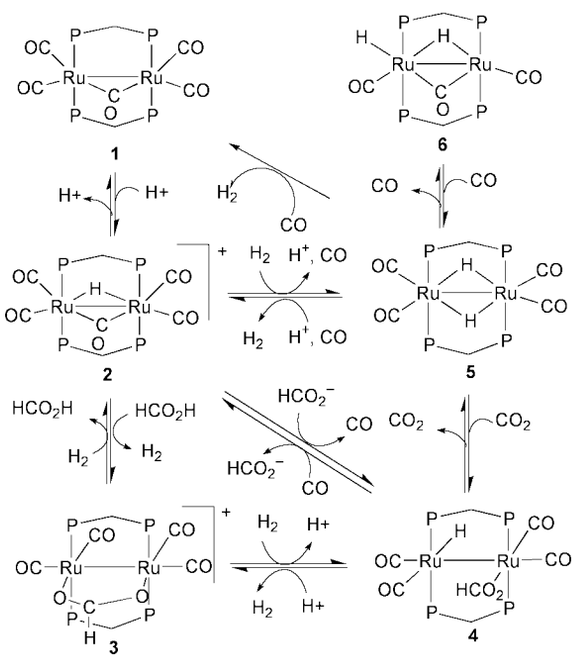

Scheme 2

and the reaction sequence is described below. At −30 °C the first complex to be observed was the cation $[Ru_2(\mu\text{-}H)(\mu\text{-}CO)(CO)_4(\mu\text{-}dppm)_2]^+$, **2**, as the formate salt. This complex is formed by protonation of the Ru–Ru bond of **1**. It was readily identified since the ^{1}H and ^{31}P NMR spectra are essentially identical to those of the known complexes **2**[BF_4] and **2**[PF_6], which are formed by protonation of **1** with HBF_4 or HPF_6 respectively.[12] In addition, it was characterized by its ^{13}C NMR spectrum, which contained three carbonyl resonances as expected for a non-fluxional complex. This is in contrast to **1**, which gives only one carbonyl resonance in the ^{13}C NMR spectrum at $\delta = 226$, indicating rapid fluxionality by a merry-go-round mechanism. Clearly the bridging hydride in **2** prevents this carbonyl migration from occurring. When a solution of **2** under ^{13}CO atmosphere was monitored by ^{13}C NMR, the ^{13}CO resonances grew in the sequence terminal CO *cis* to μ-H (about one hour), then terminal CO *trans* to μ-H, then μ-CO (about one day). We suggest that the CO exchange occurs by a dissociative mechanism, and that the carbonyls *cis* to the bridging

Table 1 A comparison of some bond distances (Å) and angles (°) in complexes **1** and **2**, using the atom numbering defined in Fig. 1

	1	**2**
Ru(1)–Ru(2)	2.903(2)	2.960(3)
C(2)–Ru(1)–Ru(2)	98.4(5)	116.5(7)
C(4)–Ru(2)–Ru(1)	86.9(5)	119.2(8)
C(2)–Ru(1)–C(3)	116(1)	99(1)
C(4)–Ru(2)–C(5)	118(1)	99(1)
C(3)–Ru(1)–C(1)	99(1)	100(1)
C(5)–Ru(2)–C(1)	108(1)	98(1)

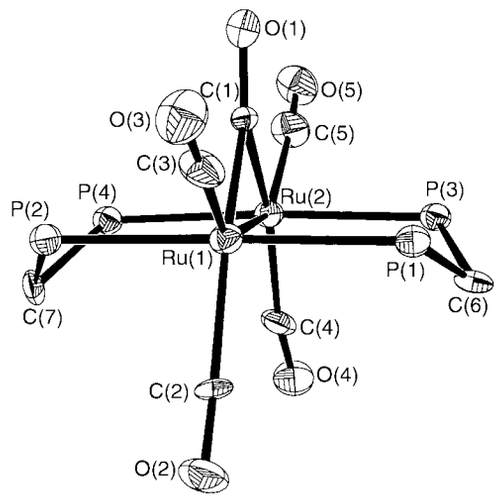

Fig. 1 A view of the structure of the cation **2** in $[Ru_2(\mu\text{-}H)(\mu\text{-}CO)(CO)_4(\mu\text{-}dppm)_2]BF_4$.

hydride are most labile. The characterization of **2** was confirmed by an X-ray structure determination of **2**[BF_4] (Fig. 1). The data were of poor quality but, though the hydride was not located, there are some interesting differences in bond parameters of **2** and **1** (Table 1).[13] Protonation of the Ru–Ru bond leads to an increase in *d*(Ru–Ru) from 2.903(2) Å in **1**[13] to 2.960(3) Å in **2**, and a corresponding opening up of the angles C(2)–Ru(1)–Ru(2) and C(4)–Ru(2)–Ru(1) by an average of 25° (Table 1), indicating that the hydride lies opposite to the bridging carbonyl and between the carbonyls C(2)–O(2) and C(4)–O(4), as expected.

The next complex to be formed in detectable quantity, at about −10 °C, was characterized as $[Ru_2(\mu\text{-}HCOO)(CO)_4(\mu\text{-}dppm)_2]^+$, **3**, also as the formate salt. At this stage the first formation of H_2 gas could be detected by ^{1}H NMR. The ^{1}H NMR data for the CH_2 protons and the ^{31}P NMR data for **3** are very similar to analogous data for the known μ-acetate analogue.[14] In addition, by using suitably ^{13}C labelled reagents, it was possible to observe the bridging H^{13}COO resonance at $\delta = 180.5$ and two resonances due to terminal carbonyl ligands at $\delta = 188$ and 206 in the ^{13}C NMR spectra. Provided the temperature did not exceed −10 °C, the catalytic decomposition of formic acid was very slow and the mixture of complexes **2** and **3** survived for at least ten hours. The reaction shown in Scheme 2 should lead to a higher equilibrium concentration of **3** relative to **2** with increasing concentration of formic acid. However, the opposite trend was observed at low temperature, indicating that equilibrium is not reached. Thus, when solutions containing complex **1** (2.2×10^{-3} M) in acetone-d_6 (0.4 mL) were reacted at −10 °C with varying amounts of formic acid (to give solutions with concentrations in the range 0.1–1 M), the NMR spectra after 0.5 hour showed that the ratio of **3**:**2** decreased as the concentration of formic acid increased and, at the higher concentrations, only **2** was present. The solution containing 1 M formic acid was allowed to warm to room temperature, when a slow reaction to give **3** and H_2 could be monitored by NMR.

The rate of catalytic decomposition of formic acid was also much slower at the higher concentrations of formic acid.

Under conditions with excess formic acid present, complexes **2** and **3** were the only complexes present in detectable quantity. As the formic acid was consumed, the catalytic decomposition accelerated and eventually complex **1** was reformed. When the reaction was monitored at 5 °C, at the stage when the formic acid was almost consumed, the concentrations of complexes **2** and **3** decreased and two transient complexes, **4** and **5**, were detected as complex **1** was regenerated. These transient complexes were characterized by their NMR spectra, but were too shortlived to allow isolation or detailed study. Complex **5** was characterized in the ^{1}H NMR spectrum by a hydride resonance at $\delta = -9.25$, which integrated as two hydrogen atoms, and by a single resonance due to methylene hydrogens of the dppm ligands at $\delta = 4.6$. The ^{31}P NMR spectrum contained a singlet resonance at $\delta = 34.3$, and the ^{13}C NMR spectrum of a ^{13}CO enriched sample gave a single resonance due to terminal carbonyl ligands at $\delta = 196.8$. These data suggest that **5** has the symmetrical structure $[Ru_2(\mu\text{-}H)_2(CO)_4(\mu\text{-}dppm)_2]$ as shown in Scheme 2. A less symmetrical but fluxional structure with terminal hydride ligands cannot be ruled out, but we note that the spectra were unchanged when the sample containing **5** was cooled to −80 °C, so any unsymmetrical structure would need to undergo very easy fluxionality. The concentration of the second transient complex **4** was never high enough to give good NMR spectra, but it was tentatively characterized as having the structure $[Ru_2H(HCOO)(CO)_4(\mu\text{-}dppm)_2]$ (Scheme 2). Complex **4** was characterized by a hydride resonance at $\delta = -6.7$ and a formyl resonance at $\delta = 8.5$ in the ^{1}H NMR spectrum, each integrating as one proton, by a formate resonance at $\delta = 165$ in the ^{13}C NMR spectrum of a sample prepared using ^{13}C labelled formic acid, and by a single resonance at $\delta = 39.85$ in the ^{31}P NMR spectrum. The concentration was too low for the carbonyl resonance(s) to be resolved in the ^{13}C NMR spectrum. The obvious problem with the suggested structure for **4** is that it should give two resonances in the ^{31}P NMR, and **4** must be fluxional in order to give the observed spectrum (eqn. (1)). Another structure that is consistent with the data is a 32-electron complex $[Ru_2(\mu\text{-}H)(\mu\text{-}HCOO)(CO)_2(\mu\text{-}dppm)_2]$.

When the catalytic decomposition of $H^{13}CO_2H$ by **1** was studied, no ^{13}CO enrichment of the carbonyl ligands of intermediates **2**–**5** or of reformed **1** was detected, so the final formation of **1** requires recoordination of CO that was displaced at the intermediate stages (Scheme 2). It is likely that this occurs by displacement of dihydrogen from intermediate **5** by free CO. When the catalytic reaction was investigated in an open system, such that the CO could escape as it dissociated, a coordinatively unsaturated dihydride $[Ru_2H(\mu\text{-}H)(\mu\text{-}CO)(CO)_2(\mu\text{-}dppm)_2]$, **6**, was detected in solution. Complex **6** reacted rapidly with carbon monoxide with loss of dihydrogen to regenerate **1**. Complex **6** was characterized by the presence of two hydride resonances in the ^{1}H NMR spectrum at $\delta = -9.3$ (terminal hydride) and −9.6 (bridging hydride), and two multiplet resonances in the ^{31}P NMR spectrum at $\delta = 42.5$ and 46.5, indicating an unsymmetrical, non-fluxional structure. It was successfully crystallized and the structure is shown in Fig. 2, with selected distances and angles in Table 2. The distance Ru–Ru = 2.8769(5) Å is shorter than in complexes **1** and **2** (Table 1) but still in the range expected for a single bond. Complex **6** is the first coordinatively unsaturated dihydridodiruthenium complex to be reported, but related 32-electron diruthenium complexes $[Ru_2(CO)_4(\mu\text{-}PNP)_2]$ and $[Ru_2(\mu\text{-}H)(\mu\text{-}CO)(CO)_3(\mu\text{-}PNP)_2]^+$ {PNP = $(i\text{-}PrO)_2PN(Et)P(Oi\text{-}Pr)_2$}, containing zero or one hydride respectively, have been characterized and have shorter Ru–Ru distances of 2.763(1) and 2.816(1) Å respectively.[15] A 30-electron complex $[Ru_2I_2(\mu\text{-}CO)_2(\mu\text{-}dppm)_2]$ is also known and has d(Ru–Ru) = 2.738(2) Å; this is suggested to be a triple bond.[16]

Table 2 Selected bond distances (Å) and angles (°) for complex **6**

Ru(1)–Ru(2)	2.8769(5)	C(1)–Ru(1)–C(2)	100.3(2)
Ru(1)–C(1)	1.857(5)	C(3)–Ru(2)–C(2)	106.2(2)
Ru(1)–C(2)	2.198(5)	Ru(1)–Ru(2)–C(3)	155.8(2)
Ru(2)–C(2)	2.006(4)	Ru(2)–Ru(1)–C(1)	144.3(2)
Ru(2)–C(3)	1.841(5)	Ru(1)–C(2)–O(2)	137.5(3)
Ru(1)–P(1)	2.330(1)	Ru(2)–C(2)–O(2)	136.3(4)
Ru(1)–P(3)	2.324(1)	P(1)–Ru(1)–P(3)	172.34(4)
Ru(2)–P(2)	2.357(1)	P(2)–Ru(2)–P(4)	172.52(4)
Ru(2)–P(4)	2.366(1)		

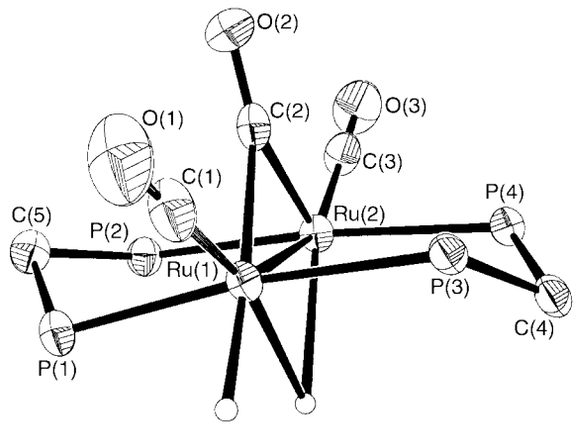

Fig. 2 A view of the structure of the coordinatively unsaturated complex $[Ru_2H(\mu\text{-}H)(\mu\text{-}CO)(CO)_2(\mu\text{-}dppm)_2]$ **6**. The hydride ligands were located in a difference map but were not refined. Approximate distances: bridging hydride, Ru(1)–H(1) = 2.16; Ru(2)–H(1) = 2.16; terminal hydride, Ru(1)–H(2) = 1.66 Å.

It is likely that **6** is formed by β-elimination of CO_2 from the formate group of the hydrido(formato) complex **4**, perhaps with CO dissociation.[17] A vacant site is needed if the CO_2 elimination occurs by a concerted mechanism.[18]

Further observations on the catalytic decomposition of formic acid

Since the rate of the catalytic reaction accelerated as the reaction proceeded, and the relative concentrations of the different diruthenium complexes present in solution changed during the reaction, it was not easy to plan a kinetic study, so tentative deductions on the mechanism are made by combining qualitative observations.

Effects of pH and solvent. There are several results that suggest that the slow step in the catalytic cycle involves addition of formate ion to a diruthenium complex. These are as follows. (1) The addition of triethylamine to the reaction mixture accelerates the decomposition of formic acid. Under these conditions slow catalytic decomposition could be observed over the temperature range of −10 to −30 °C. Also, under these conditions, the concentrations of the transient complexes **5** and **4** were higher near the end of the catalytic decomposition. The neutral complexes **1**, **4** and **5** are only present in detectable amounts when the concentration of formic acid is low, since each reacts easily with a proton to yield a cationic complex (Scheme 2). (2) The catalytic reaction is slower at higher concentration of formic acid, and so accelerates as the reaction proceeds. The concentration of free formate is greatly decreased in formic acid by formation of the adduct $[(HCO_2)_2H]^-$ and so, if free formate ion is needed in a key step, the reaction is slower in more acidic solution.[19] (3) The reaction is completely suppressed in the presence of triflic acid (6 : 1 ratio of formic acid : triflic acid was used). No detectable decomposition of formic acid occurred over one day in acetone solution at room temperature under conditions when the reaction with formic acid alone was complete in minutes. The only complex present in solution in

Table 3 Catalysis of formation of formic acid by the hydrogenation of CO_2 by complex **1**

Run	P^a/psi	[Catalyst **1**]/10^{-3} mmol	Et_3N/mL	[HCOOH]/mmol	Time/h	TON	TOF^b/h^{-1}
1	560	59.4^c	15	4.6	1	77	77
2	560	59.4^c	15	31	4	520	130
3	560	59.4^c	15	62	9	1050	116
4	560	59.4^c	15	65	21	1100	52
5	1020	59.4^c	15	12	1	207	207
6	1020	59.4^c	15	128	21	2160	103
7	1020	99^d	0	17	48	176	4

^{a} P = total pressure; $p(H_2) = p(CO_2)$ in each experiment. ^{b} TOF is the turnover frequency, TOF = TON/time. ^{c} Solvent acetone (30 mL). ^{d} Solvent acetone (50 mL).

the presence of triflic acid was complex **2**. Again, this is consistent with free formate being needed for the decomposition. (4) The catalytic reaction is much faster in the dipolar, aprotic solvent acetone than in dichloromethane or toluene. This suggests that attack by formate on a cationic diruthenium complex, for example the conversion of **2** to **4** in Scheme 2, might be the slow step or involved in an important equilibrium step.

Importance of vacant sites. There are several observations which indicate that coordinative unsaturation at the diruthenium centre is either necessary or at least advantageous at some stages of reaction. The catalytic reaction is completely inhibited when carried out under an atmosphere of carbon monoxide. Under these conditions, reaction proceeded only to give a mixture of **2** and **3** at room temperature. If the carbon monoxide was swept from the system by a flow of nitrogen, the decomposition of formic acid began. Similarly, the catalytic reaction was inhibited by addition of phenylacetylene, which can bind to the diruthenium centre.[20] If the catalysis was carried out in a vessel from which gaseous products could escape, the coordinatively unsaturated complex **6** could be detected in solution when the formic acid was completely decomposed. Addition of more formic acid led to very rapid catalytic decomposition, indicating that **6** is a much more active catalyst precursor than the coordinatively saturated complex **1**.

Labelling studies. The catalytic decomposition of formic acid proceeds to completion and the back reaction is negligible under the reaction conditions used. This was shown by monitoring the decomposition of DCO_2H to give a mixture of CO_2, H_2, HD and D_2. No resonance for the formyl proton of HCO_2D, which would be formed by the back reaction, was detected at intermediate stages. Similarly, HCO_2D failed to give DCO_2H at intermediate stages. These observations are not unexpected since the equilibrium strongly favors the products CO_2 and hydrogen under the conditions used.[4,5]

When the reaction of **1** with HCOOD/D_2O in acetone-d_6 was monitored by ^{1}H NMR at low temperature (−10 to −30 °C), complex **2** still exhibited a hydride resonance at $\delta = -8.9$ and its intensity was considerably higher than expected based on the proton impurity in the formic acid-d_1. Independent experiments showed that exchange between the OD deuterium atoms of HCOOD and D_2O is slow at −10 °C, since separate resonances were observed in the ^{2}H NMR spectrum in acetone at $\delta = 10.9$ and at $\delta = 3.8$ respectively. However, on addition of complex **1**, the peaks coalesced and only a single resonance was observed at $\delta = 8.0$ under the same conditions. This proton exchange is probably catalysed by the formate ion that is formed on formation of complex **2**. It seems that there is an equilibrium isotope effect that favours formation of $[Ru_2(\mu\text{-H})(\mu\text{-CO})(CO)_4(\mu\text{-dppm})_2]^+$, **2**, rather than $[Ru_2(\mu\text{-D})(\mu\text{-CO})(CO)_4(\mu\text{-dppm})_2]^+$, **2**-$d_1$, and that H–D exchange with proton impurities in the solvent medium provides a proton source.

Mass spectrometric analysis of the gases formed by decomposition of HCOOD or DCOOH showed that the hydrogen formed at the end of the reaction was an approximately 1 : 2 : 1 mixture of H_2, HD and D_2, as expected from statistical considerations. This observation is inconsistent with an entirely intramolecular mechanism, which should give HD only. However, catalytic decomposition of HCOOH in the presence of D_2 gave both H_2 and HD, showing that dihydrogen can be activated by one or more of the catalytic intermediates (Scheme 2), so it is possible that HD scrambling in the dihydrogen product might occur after the primary decomposition.

Analysis of the hydrogen formed by reaction of **1** with HCO_2D at −7 °C to give a mixture of **2**, **3** and dihydrogen (Scheme 2) showed that it contained an approximately 2 : 1 ratio of H_2:HD. This is consistent with the observation of the hydride resonance for **2**, and is attributed to a large isotope effect coupled with H–D exchange between the formic acid-*d* and protic impurities in the acetone-d_6 solvent (see above), but it gives little further mechanistic insight.

Hydrogenation of CO_2 to formic acid

It is expected, and has been observed in several instances, that catalysts for the decomposition of formic acid to CO_2 and H_2 should also catalyze the hydrogenation of CO_2 to formic acid.[7,8] Complex **1** is indeed an active catalyst for formation of formic acid. The reactions were carried out at room temperature in acetone solvent with excess triethylamine present to stabilize the formic acid.[4,5] Equal pressures of carbon dioxide and hydrogen were used and reactions were carried out using a stainless steel pressure reactor, fitted with a pressure gauge to monitor the reaction. The pressure decreased as reaction occurred to finally give a constant equilibrium value. More accurate values of the conversion to formic acid were obtained by cooling the vessel rapidly to quench the reaction, releasing the pressure, and then determining the concentration of formate by NMR analysis at a sufficiently low temperature (−20 °C) that the back reaction did not occur. The results are given in Table 3.

The first four entries in Table 3 show that the reaction is complete in about nine hours at room temperature under the conditions used. The turnover number and frequency were 1050 and 116 h^{-1} under these conditions. There was little further change after 21 h reaction. The activity is comparable to the best mononuclear complex catalysts, such as $[Rh(Ph_2PCH_2CH_2PPh_2)(CF_3COCHCOCF_3)]$ which gives TOF = 170 h^{-1} at 25 °C in DMSO/Et_3N or $[RuH_2(PMe_3)_4]$ which gives TOF = 630 h^{-1} in supercritical CO_2 at 50 °C.[4–8] When the pressure was increased to 1020 psi, the yield of formic acid was significantly higher, as found with other systems (runs 5 and 6, Table 3).[8,20] The yield of formic acid was much lower in the absence of triethylamine, as expected (run 7, Table 3).[4,5]

Evaporation of the solution obtained after a catalytic reaction gave back the starting complex **1** in high yield. Analysis of the catalytic solution by ^{31}P NMR at room temperature immediately after release of the pressure showed that a mixture

of complexes **1**, **2** and **3** was present. In the absence of Et_3N (run 7, Table 3), the only ruthenium complex present in solution after the release of the pressure was complex **2** and it was stable even at room temperature. This is expected since complex **2** is stabilized in the presence of excess formic acid. All these data indicate that the mechanism of formation of formic acid is the reverse of that for its decomposition.

Discussion

The reactions of Scheme 2 provide a possible mechanism for the equilibration between formic acid and H_2/CO_2, but there are some problems which should be discussed. In acid solution, complex **2** is thermally stable. In principle, the equilibrium should favor formation of **3** under acid conditions and so it is likely that **2** is kinetically stable under these conditions. It is likely that **3** is formed by way of **4** which requires free formate ion to occur. The neutral hydrides **4**, **5** and **6** are not observed in acid solution presumably because each reacts rapidly with protons. The result is that the resting state of the catalyst depends critically on pH and hence on the extent of the catalytic reaction to form or destroy formic acid.

The observation of very strong retardation by free CO suggests that coordinatively unsaturated complexes may be important in the catalysis. Complex **6** is observed under experimental conditions in which CO can escape from the reaction mixture during decomposition of formic acid, and other unsaturated intermediates might well be involved but are not observed. Scheme 2 requires loss of CO_2 from complex **4** to give **5** but there is no vacant site at ruthenium for the β-elimination of carbon dioxide, so this reaction would need to take place by transient dissociation of formate followed by hydride abstraction. A coordinatively unsaturated complex could give a transient carbon dioxide complex *via* β-elimination. A possible mechanism is then shown in Scheme 3. The nature of any CO_2

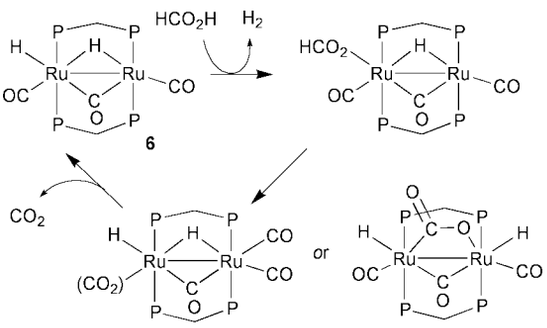

Scheme 3 A possible mechanism of catalysis.

complex is speculative, but we note that a stable complex $[Ru_2(\mu\text{-}CO_2)(CO)_4\{\mu\text{-}(EtO)_2PNEtP(OEt)_2\}_2]$ with bridging CO_2 has been reported.[21] Scheme 3 does not explicitly account for the remarkable effect of acid on the rate of reaction, but it must be noted that strong acid will destroy complex **6**, and so remove it from the catalytic cycle.

Experimental

All manipulations were carried out under a dry nitrogen atmosphere using either standard Schlenk techniques or a glove box. Solvents were dried and distilled immediately before use. The following reagents were used as purchased (note that formic acid contained 4–5% water): HCOOH (96%, H_2O 4%); DCOOH (95%, H_2O 5%), HCOOD (95%, D_2O 5%) and $H^{13}COOH$ (95%, H_2O 5%, 99 atom% C^{13}); ^{13}CO (99% ^{13}C); carbon dioxide (99.5%); hydrogen (prepurified, 99.99%). $[Ru_2(\mu\text{-}CO)(CO)_4(\mu\text{-}dppm)_2]$ was synthesized according to the literature procedure.[10] ^1H, ^{13}C, and ^{31}P NMR spectra were recorded by using a Varian Gemini 300 spectrometer. Mass spectra were recorded using a Finnigan MAT 8200 spectrometer.

NMR studies on the decomposition of formic acid

In a glove-box, a saturated acetone-d_6 solution of $[Ru_2(\mu\text{-}CO)(CO)_4(\mu\text{-}dppm)_2]$ (2.2×10^{-3} M) was prepared and a known volume was transferred by syringe into an NMR tube. The tube was then sealed with a septum. The tube was placed in the NMR probe and equilibrated to the desired temperature for 20 min, then a known volume of formic acid was added by microsyringe through the septum, and NMR spectra were recorded as the reaction proceeded. For example, in the quenching experiment using triflic acid, the triflic acid (0.5 μL) was added first followed by formic acid (3 μL).

^{13}CO labelling studies on the decomposition of formic acid

A saturated solution of $[Ru_2(\mu\text{-}CO)(CO)_4(\mu\text{-}dppm)_2]$ in acetone-d_6 (0.9 mL, 2.2 mM) in an NMR tube was prepared in a glove-box, and sealed as above. Excess ^{13}CO was introduced into the tube by syringe, and the solution was allowed to equilibrate for 15 h. The reaction with formic acid was then monitored as above.

MS studies on the decomposition of formic acid

A saturated solution of $[Ru_2(\mu\text{-}CO)(CO)_4(\mu\text{-}dppm)_2]$ in acetone-d_6 (0.9 mL, 2.2 mM) in an NMR tube was prepared as above, then cooled to −7 °C. Formic acid (3 μL) was added by syringe, and MS spectra were recorded immediately from a sample (0.5 mL) of the gas phase. Further samples were analysed in the same way.

Hydrogenation of CO_2 to formic acid

A stainless steel autoclave (350 mL), fitted with a stirrer, temperature controller and pressure gauge, was charged with a saturated solution of $[Ru_2(\mu\text{-}CO)(CO)_4(\mu\text{-}dppm)_2]$ in acetone (30 mL, 2.2 mM) and Et_3N (15 mL) under a nitrogen atmosphere. CO_2 was passed into the autoclave for 10 min at room temperature to displace the nitrogen and the pressure of CO_2 was then raised to the desired value. An equal pressure of hydrogen was then added and the autoclave was sealed. After the desired reaction time, the autoclave was cooled to −30 °C for 15 min and the pressure was then released. A sample of the solution (0.5 mL) was transferred to an NMR tube containing acetone-d_6 (0.9 mL) and kept at −20 °C (to prevent the back reaction from occurring), for ^1H NMR analysis. The concentration of formic acid was determined from the integral of the signal of the formyl proton at $\delta = 8.1$, by comparison with the resonance of Et_3N at $\delta = 3.2$ or of the CH_2 protons of dppm in compound **2** at $\delta = 4.1$ and 4.3.

Characterization of intermediates formed during the decomposition of formic acid

$[Ru_2(\mu\text{-}H)(\mu\text{-}CO)(CO)_4(\mu\text{-}dppm)_2][HCOO]$, 2$[HCO_2]$. To a saturated solution of $[Ru_2(\mu\text{-}CO)(CO)_4(\mu\text{-}dppm)_2]$ in acetone-d_6 (0.5 mL, 2.2 mM) in an NMR tube at room temperature was added HCOOH (15 μL) to give a solution containing pure **2**$[HCO_2]$. NMR in acetone-d_6: $\delta(^1H) = 8.4$ [s, $HCOO^-$]; 4.14, 4.48 [m, 4H, CH_2P_2]; −8.93 (quin, 1H, $^2J(PH) = 9.2$ Hz, HRu]; $\delta(^{31}P) = 27.8$ [s, dppm]; for sample prepared by reaction of formic acid (15 μL) with ^{13}CO labelled $[Ru_2(\mu\text{-}CO)(CO)_4(\mu\text{-}dppm)_2]$, $\delta(^{13}C) = 198.6$ [m, terminal CO]; 201 [s, terminal CO]; 278.6 [m, μ-CO]. A solution containing pure **2** could also be prepared by adding HCOOH (3 μL) to a solution of $[Ru_2(\mu\text{-}CO)(CO)_4(\mu\text{-}dppm)_2]$ (15 mg) in CD_2Cl_2 (0.5 mL). The NMR parameters were very similar to those above.

$[Ru_2(\mu\text{-}HCOO)(CO)_4(\mu\text{-}dppm)_2][HCOO]$, 3[HCOO]. The highest concentration of complex **3**, as a mixture with complex

Table 4 Crystal data for complexes **2**[BF_4] and **6**·2Me_2CO

Complex	**2**[BF_4]	**6**·2Me_2CO
Formula	$C_{55}H_{45}BF_4O_5P_4Ru_2$	$C_{59}H_{58}O_5P_4Ru_2$
M	1197.73	1174.08
Temperature/K	295(2)	296(2)
Crystal system, space group	Monoclinic, $P2_1/c$	Monoclinic, $P2_1/n$
a/Å	12.437(1)	11.583(1)
b/Å	17.804(3)	28.557(3)
c/Å	27.390(4)	16.783(2)
β/°	92.511(8)	97.817(1)
Volume/Å^3, Z	6059(1), 4	5499.7(9), 4
ρ/Mg m^{-3}	1.313	1.417
μ/mm^{-1}, F(000)	0.657, 2412	0.713, 2400
Independent reflections	6280	9478
Data/restraints/parameters	5208/0/620	9473/0/637
$R1$, $wR2$ ($I > 2\sigma(I)$)	0.115, 0.329	0.0466, 0.0918

2, was obtained by addition of HCOOH (1.5 μL) to a saturated solution of [Ru_2(μ-CO)$(CO)_4$(μ-dppm)$_2$] in acetone-d_6 (0.7 mL, 2.2 mM) in an NMR tube at −10 °C. NMR in acetone-d_6: $\delta(^1H) = 8.4$ [s, HCOO]; 4.45, 4.90 [m, 4H, $^2J(HH) = 15$ Hz, $^2J(PH) = 5$ Hz, CH_2P_2]; $\delta(^{31}P) = 30.9$ [s, dppm]; for samples prepared using H^{13}COOH or ^{13}CO labelled [Ru_2(μ-CO)$(CO)_4$(μ-dppm)$_2$], $\delta(^{13}C) = 180.5$ [s, HCO_2]; 188 [m, terminal CO]; 206 [s, terminal CO].

[Ru_2(μ-H)$_2(CO)_4$(μ-dppm)$_2$], 5 and [Ru_2(H)(HCOO)$(CO)_4$-(μ-dppm)$_2$], 4. To a saturated solution of [Ru_2(μ-CO)$(CO)_4$-(μ-dppm)$_2$] in acetone-d_6 (0.9 mL, 2.2 mM) in an NMR tube at −10 °C was added HCOOH (3 μL). The reacting solution was monitored by NMR at ¯10 °C. For a brief period, when the formic acid was almost consumed, complex **5** became the dominant species. The solution was quickly cooled to −30 °C and NMR spectra were recorded. NMR in acetone-d_6: $\delta(^1H) = 4.6$ (quin, 4H, CH_2P_2); −9.25 (quin, 2H, $^2J(PH) = 9.2$ Hz, HRu); $\delta(^{31}P) = 34.3$ [s, dppm]; for a sample prepared from ^{13}CO labelled [Ru_2(μ-CO)$(CO)_4$(μ-dppm)$_2$], $\delta(^{13}C) = 196.8$ [s, terminal CO].

Complex **4** was observed along with complex **5** and was stable for a very limited time. NMR in acetone-d_6: $\delta(^1H) = 8.5$ [s, HCOO]; −6.7 [br, RuH]; $\delta(^{13}C) = 165$ (s, formate, ^{13}C labelled sample); $\delta(^{31}P) = 39.85$ [s, dppm].

[Ru_2H(μ-H)(μ-CO)$(CO)_2$(μ-dppm)$_2$], 6. To a solution/suspension of [Ru_2(μ-CO)$(CO)_4$(μ-dppm)$_2$] (0.1 g) in acetone-d_6 (0.5 mL) in an NMR tube at room temperature was added HCOOH (15 μL). A pin-hole in the NMR cap allowed gases to escape. After 1 day, the NMR spectrum indicated formation of **6** and red crystals precipitated slowly. NMR in acetone-d_6: $\delta(^1H) = 3.71$, 3.82 [m, 4H, CH_2P_2]; −9.3 [t, 1H, $^2J(PH) = 9$ Hz, HRu]; −9.6 (quin, 1H, $^2J(PH) = 9$ Hz, HRu_2]; $\delta(^{31}P) = 42.5$, 46.5 [m, dppm]. Yield 0.02 g. Calc. for $C_{53}H_{46}O_3P_4Ru_2$: C, 60.3; H, 4.4. Found: C, 60.4, H, 4.6%. Complex **6** was stable as a solid but it decomposed rapidly on redissolution in the absence of hydrogen.

X-Ray structure determinations

Crystals of **2**[BF_4] were grown from acetone/pentane solution. Data were collected at room temperature by using an Enraf-Nonius diffractometer fitted with a CCD detector. The crystal diffracted only weakly; hence the R factor is high and standard deviations on the bond parameters are large. A semi-empirical absorption correction was applied using ψ scans. The space group was determined by systematic absences and the structure was solved using direct methods and refined by full-matrix least-squares procedures based on F^2 using the SHELXTL software package.[22] Crystals of **6**·2Me_2CO were obtained from acetone solution. Data were collected at room temperature by using a Bruker AX SMART 1k CCD diffractometer. The absorption correction, solution and refinement were carried out in a similar way as above. Crystal data are given in Table 4.

CCDC reference number 186/2112.

See http://www.rsc.org/suppdata/dt/b0/b004234j/ for crystallographic files in .cif format.

Acknowledgements

We thank the NSERC (Canada) for financial support.

References

1 A. Fujii, S. Hashiguchi, N. Uematsu, T. Ikariya and R. Noyori, *J. Am. Chem. Soc.*, 1996, **118**, 2521.
2 N. Uematsu, A. Fujii, S. Hashiguchi, T. Ikariya and R. Noyori, *J. Am. Chem. Soc.*, 1996, **118**, 4916.
3 K. Matsumura, S. Hashiguchi, T. Ikariya and R. Noyori, *J. Am. Chem. Soc.*, 1997, **119**, 8738.
4 P. G. Jessop, T. Ikariya and R. Noyori, *Chem. Rev.*, 1995, **95**, 260; P. G. Jessop, T. Ikariya and R. Noyori, *Chem. Rev.*, 1999, **99**, 475.
5 W. Leitner, *Angew. Chem., Int. Ed. Engl.*, 1995, **34**, 2207.
6 P. G. Jessop, Y. Hsiao, T. Ikariya and R. Noyori, *J. Am. Chem. Soc.*, 1996, **118**, 344.
7 F. Hutschka, A. Dedieu, M. Eichberger, R. Fornika and W. Leitner, *J. Am. Chem. Soc.*, 1997, **119**, 4432.
8 J. C. Tsai and K. M. Nicholas, *J. Am. Chem. Soc.*, 1992, **114**, 5117.
9 Y. Gao, J. Kuncheria, G. P. A. Yap and R. J. Puddephatt, *Chem. Commun.*, 1998, 2365.
10 H. A. Mirza, J. J. Vittal and R. J. Puddephatt, *Inorg. Chem.*, 1993, **32**, 1327.
11 (*a*) R. S. Coffey, *Chem. Commun.*, 1967, 923; (*b*) S. H. Strauss, K. H. Whitmire and D. F. Shriver, *J. Organomet. Chem.*, 1979, **174**, C59; (*c*) R. S. Paonessa and W. C. Trogler, *J. Am. Chem. Soc.*, 1982, **104**, 3529.
12 (*a*) J. S. Field, R. J. Haines, C. N. Sampson and J. Sundermeyer, *J. Organomet. Chem.*, 1987, **322**, C7; (*b*) J. S. Field, R. J. Haines, E. Minshall, C. N. Sampson and J. Sundermeyer, *J. Organomet. Chem.*, 1987, **327**, C18; (*c*) J. S. Field, R. J. Haines, E. Minshall, C. N. Sampson, J. Sundermeyer and S. F. Woollam, *J. Chem. Soc., Dalton Trans.*, 1992, 2624.
13 (*a*) J. Kuncheria, H. A. Mirza, H. A. Jenkins, J. J. Vittal and R. J. Puddephatt, *J. Chem. Soc., Dalton Trans.*, 1998, 285; (*b*) G. M. Ferrence, P. E. Fanwick, C. P. Kubiak and R. J. Haines, *Polyhedron*, 1997, **16**, 1453.
14 S. J. Sherlock, M. Cowie, E. Singleton and M. M. D. V. Steyn, *Organometallics*, 1988, **7**, 1663.
15 (*a*) K. J. Edwards, J. S. Field, R. J. Haines, B. D. Homann, M. W. Stewart, J. Sundermeyer and S. F. Woollam, *J. Chem. Soc., Dalton Trans.*, 1996, 4171; (*b*) J. S. Field, R. J. Haines, J. Sundermeyer and S. F. Woollam, *J. Chem. Soc., Dalton Trans.*, 1993, 947.
16 K.-B. Shiu, S.-S. Young, S.-I. Chen, J.-Y. Chen, H.-J. Wang, S.-L. Wang, F.-L. Liao, S.-M. Peng and Y.-L. Liu, *Organometallics*, 1999, **18**, 4244.
17 Loss of CO is required if the structure shown in Scheme 2 is correct, but note that the structure of **4** is not rigorously established.
18 The reversible insertion of CO_2 into an M–H bond to give formate, may occur by migratory insertion requiring a vacant site, or by direct hydride attack on the carbon atom of CO_2. D. J. Darensbourg, H. P. Wiegreffe and P. W. Wiegreffe, *J. Am. Chem. Soc.*, 1990, **112**, 9252.
19 Y. P. Pan and M. A. McAllister, *J. Am. Chem. Soc.*, 1998, **120**, 166.
20 E. Linder, B. Keppeler and P. Wegner, *Inorg. Chim. Acta*, 1997, **258**, 97.
21 J. S. Field, R. J. Haines, J. Sundermeyer and S. F. Woollam, *J. Chem. Soc., Dalton Trans.*, 1993, 2735.
22 SHELXTL, Siemens Analytical X-Ray Instruments, Madison, WI, 1994.